

OPEN ACCESS

EDITED BY

Manoj Baranwal,
Thapar Institute of Engineering
& Technology, India

REVIEWED BY

Kuanhui Xiang,
School of Basic Medical Sciences,
Peking University, China
Amilcar Tanuri,
Federal University of Rio de Janeiro,
Brazil
Chaitanya Kurhade,
University of Texas Medical Branch at
Galveston, United States
Jun Wang,
Rutgers, The State University of New
Jersey, United States

*CORRESPONDENCE

Vladimir Leksa
vladimir.leksa@savba.sk
Anna Ohradanova-Repic
anna.repic@meduniwien.ac.at

SPECIALTY SECTION

This article was submitted to
Viral Immunology,
a section of the journal
Frontiers in Immunology

RECEIVED 31 May 2022

ACCEPTED 03 August 2022

PUBLISHED 23 August 2022

CITATION

Ohradanova-Repic A, Skrabana R,
Gebetsberger L, Tajti G, Baráth P,
Ondrovičová G, Praženicová R,
Jantova N, Hrasnova P, Stockinger H
and Leksa V (2022) Blockade of
TMPRSS2-mediated priming of
SARS-CoV-2 by lactoferricin.
Front. Immunol. 13:958581.
doi: 10.3389/fimmu.2022.958581

COPYRIGHT

© 2022 Ohradanova-Repic, Skrabana,
Gebetsberger, Tajti, Baráth,
Ondrovičová, Praženicová, Jantova,
Hrasnova, Stockinger and Leksa. This is
an open-access article distributed under
the terms of the [Creative Commons
Attribution License \(CC BY\)](https://creativecommons.org/licenses/by/4.0/). The use,
distribution or reproduction in other
forums is permitted, provided the
original author(s) and the copyright
owner(s) are credited and that the
original publication in this journal is
cited, in accordance with accepted
academic practice. No use,
distribution or reproduction is
permitted which does not comply with
these terms.

Blockade of TMPRSS2-mediated priming of SARS-CoV-2 by lactoferricin

Anna Ohradanova-Repic^{1*}, Rostislav Skrabana²,
Laura Gebetsberger¹, Gabor Tajti¹, Peter Baráth³,
Gabriela Ondrovičová⁴, Romana Praženicová^{4,5},
Nikola Jantova^{2,5}, Patricia Hrasnova^{2,5}, Hannes Stockinger¹
and Vladimir Leksa^{1,4*}

¹Medical University of Vienna, Center for Pathophysiology, Infectiology and Immunology, Institute for Hygiene and Applied Immunology, Vienna, Austria, ²Laboratory of Structural Biology of Neurodegeneration, Institute of Neuroimmunology, Slovak Academy of Sciences, Bratislava, Slovakia, ³Department of Glycobiology, Institute of Chemistry, Slovak Academy of Sciences, Bratislava, Slovakia, ⁴Laboratory of Molecular Immunology, Institute of Molecular Biology, Slovak Academy of Sciences, Bratislava, Slovakia, ⁵Department of Biochemistry, Comenius University, Bratislava, Slovakia

In addition to vaccines, there is an urgent need for supplemental antiviral therapeutics to dampen the persistent COVID-19 pandemic caused by the severe acute respiratory syndrome coronavirus-2 (SARS-CoV-2). The transmembrane protease serine 2 (TMPRSS2), that is responsible for proteolytic priming of the SARS-CoV-2 spike protein, appears as a rational therapeutic target. Accordingly, selective inhibitors of TMPRSS2 represent potential tools for prevention and treatment of COVID-19. Previously, we identified the human milk glycoprotein lactoferrin as a natural inhibitor of plasminogen conversion to plasmin, a serine protease homologous to TMPRSS2. Here, we tested whether lactoferrin and lactoferricin, a biologically active natural peptide produced by pepsin-mediated digestion of lactoferrin, together with synthetic peptides derived from lactoferrin, were able to block TMPRSS2 and SARS-CoV-2 infection. Particularly, we revealed that both lactoferricin and the N-terminal synthetic peptide pLF1 significantly inhibited: i) proteolytic activity of TMPRSS2 and plasmin, ii) proteolytic processing of the SARS-CoV-2 spike protein, and iii) SARS-CoV-2 infection of SARS-CoV-2-permissive cells. Thus, natural and synthetic peptides derived from lactoferrin represent feasible candidates for supporting prevention and treatment of COVID-19.

KEYWORDS

COVID-19, SARS-CoV-2, coronavirus, virus priming, serine proteases, TMPRSS2, lactoferrin, lactoferricin

Abbreviations: ACE2, angiotensin converting enzyme-2; Ap, aprotinin; COVID-19, coronavirus disease 2019; HSPGs, heparan sulfate proteoglycans; LF, lactoferrin; LFC, lactoferricin; mAb, monoclonal antibody; Plg, plasminogen; SARS-CoV-1, severe acute respiratory syndrome coronavirus 1; SARS-CoV-2, severe acute respiratory syndrome coronavirus 2; TMPRSS2, transmembrane protease serine 2; uPA, urokinase-type plasminogen activator.

Introduction

The global COVID-19 pandemic is unceasingly firing up a demand for cheap and available therapeutics to supplement standard treatment protocols. The angiotensin converting enzyme-2 (ACE2) serves as a dominant host cell-surface receptor for the severe acute respiratory syndrome coronavirus-2 (SARS-CoV-2) through engagement of the viral spike (S) protein (1, 2), although additional interaction sites in virus-cell attachment have been suggested, including heparan sulfate proteoglycans (HSPGs) (3). Upon binding, proteolytic processing of the S protein, i.e. virus priming (4, 5), by host serine proteases, in particular by the transmembrane protease serine 2 (TMPRSS2) (6), is essential for fusion of viral and cellular membranes, and subsequent virus entry to the host cell.

Colocalization of ACE2 and TMPRSS2, a canonical priming protease of both SARS-CoV-1 and SARS-CoV-2, is crucial for viral infection of target cells. S protein interacts with ACE2 *via* its N-terminal moiety (S1) encompassing the receptor-binding domain (RBD), and then is cleaved by proximal TMPRSS2 at the site between S1 and the C-terminal moiety (S2). This initial cleavage is followed by cleavage at the S2' site, which reveals the Ser816-Phe833 fusion peptide and triggers a fusion of viral membrane with the host cell membrane (4, 5). Thus, the inhibition of each event, virus binding, priming and fusion, represents a promising piece in the puzzle of managing the COVID-19 pandemic (7–9).

Active sites of several human serine proteases exhibit high identity with TMPRSS2, the one of plasminogen even 95% (10). Previously, we identified the human milk glycoprotein lactoferrin (LF) as an inhibitor of the proteolytic conversion of plasminogen to plasmin (11). Here, we expand these data to TMPRSS2. In addition to full-length LF, we tested its N-terminal bioactive peptide called lactoferricin (LFC), which is known for its antiviral and antibacterial activities. LFC is physiologically produced from the N-terminal region of LF upon cleavage by pepsin (12, 13). In a similar way, we produced LFC *in vitro*. We show that LFC and the corresponding synthetic peptide pLF1 designed by us from the N-terminal region of LF inhibit TMPRSS2, and subsequently, SARS-CoV-2 priming and infection of target cells.

Results

Previously, we described the binding of lactoferrin (LF) to plasminogen (Plg), which blocked Plg conversion to the active serine protease plasmin. According to our mapping studies, LF bound to Plg *via* its highly cationic N-terminal region (11). Since structures of the catalytic domains of serine proteases display a high level of identity (10), we have tested the inhibitory effect of LF and three LF-derived synthetic peptides against other serine proteases, including TMPRSS2, elastase and trypsin, in addition

to plasmin. The peptides we used were as follows: pLF1 from the N-terminal region, pLF2 from the helix linker region, and pLF3 from the C-terminal region (11). Additionally, we used peptide pCTR as a negative control (11) and the broad-spectrum serine protease inhibitor aprotinin as a positive control.

An *in vitro* proteolysis assay at 37°C using the fluorogenic serine protease substrate Boc-Gln-Ala-Arg-AMC revealed that pLF1, but neither full-length LF nor other tested peptides derived from LF, nor the control peptide pCTR, significantly reduced the proteolytic activity of TMPRSS2 (Figure 1A), plasmin or elastase (Figures 1B, C). The inhibitory effect of pLF1 on trypsin was not significant (Figure 1D). pLF1 inhibited TMPRSS2 with the half-maximum inhibitory concentration (IC₅₀) of 9.8 µg/mL, with maximum inhibition at 40 - 80 µg/mL, approaching a plateau of ~ 40% inhibition (Figure 1A, *inset*). For plasmin, the IC₅₀ was 6.9 µg/mL, with maximum inhibition observed at 20 µg/mL (Figure 1B, *inset*). In contrast, full-length LF exhibited no dose-dependent inhibition of either TMPRSS2 or active plasmin (Figures 1A, B, *insets*). The competitive inhibitor aprotinin blunted the proteolytic activity of both proteases (Figures 1A, B, *insets*). Thus, while LF apparently blocked only the conversion of inactive Plg to the active serine protease plasmin (11), the N-terminal peptide pLF1 is able to execute its inhibitory effect on already active TMPRSS2, plasmin, and elastase, which implies that pLF1 may directly target the catalytic domain of serine proteases (Figures 2D).

TMPRSS2 was shown to process the S protein of the pathogenic coronaviruses SARS-CoV-1 and SARS-CoV-2 and, as a consequence, to play a central role in the coronavirus entry into a host cell (14–17). When we exposed the recombinant SARS-CoV-2 S protein to TMPRSS2 *in vitro*, we found that the S protein was cleaved by TMPRSS2 to a diffuse fragment of about 75 kD (Figure 2A) that agreed with the molecular size of the S2 domain of SARS-CoV-2 (18, 19). When we added pLF1 to the reaction, the cleavage was blocked; no such effect was seen with pCTR (Figures 2A, B). The incubation of the S protein with plasmin produced more bands within this size range, which might indicate that processing by plasmin was not as specific as by TMPRSS2. The cleavage by plasmin was also hindered in the presence of pLF1 (Figures 2C, D). When we performed the *in vitro* proteolysis assay with the S protein mutated at the S1/S2 site, we did not observe any cleavage by TMPRSS2 and only a minor cleavage with plasmin, which further supported the assumption that plasmin was less specific (Figures 2E–G). Together, these data indicate that the N-terminal fragment of LF can inhibit the proteolytic processing of the SARS-CoV-2 S protein.

To test the capacity of LF or LF-derived peptides to inhibit SARS-CoV-2 infection, we selected Vero cells, which, in contrast to Vero E6 cells, express detectable amounts of TMPRSS2 (20). Before replication-competent SARS-CoV-2 was added, the Vero cells were pre-incubated with LF, the LF-derived peptides or control pCTR for 40–60 min. As shown in Figure 3A, the N-

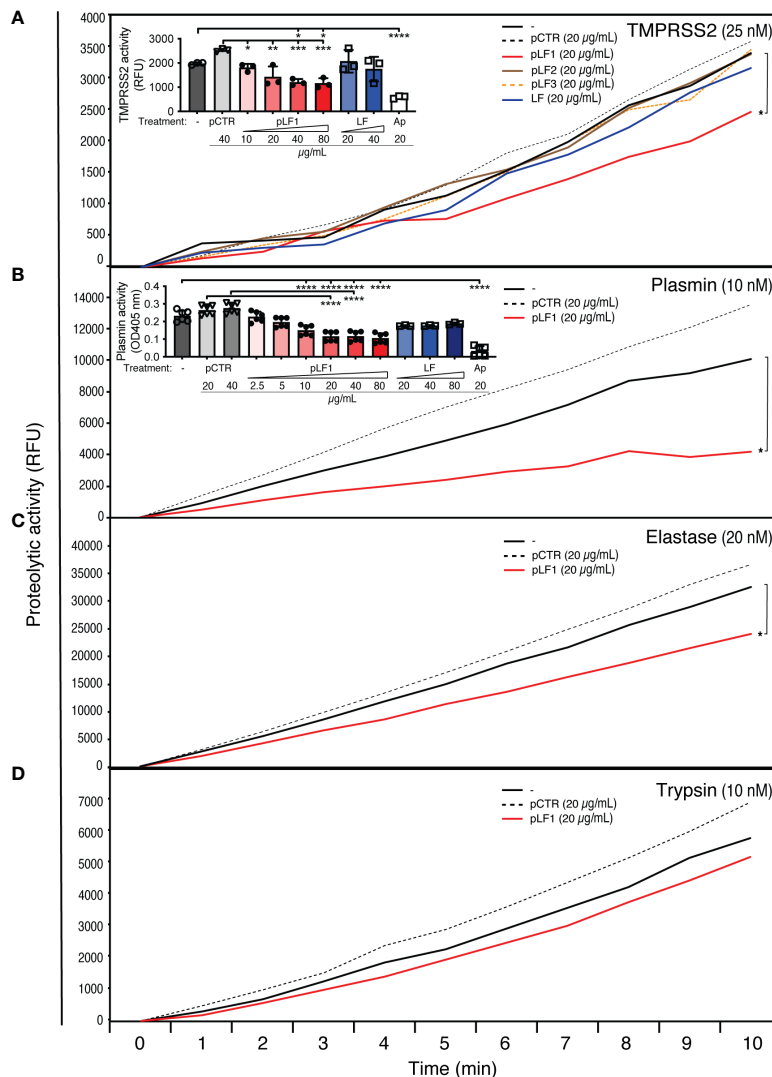


FIGURE 1

Effect of LF and the LF-derived peptides pLF1–pLF3 on the activity of serine proteases. Proteolytic activities of purified TMPRSS2 (A), plasmin (B), elastase (C), and trypsin (D) were measured with or without peptides pLF1, pLF2, pLF3, LF or the control peptide pCTR at 37°C in Tris-HCl buffer using the fluorogenic substrate Boc-Gln-Ala-Arg-AMC. The reaction was monitored using an ELISA reader for the indicated time intervals. The insets in (A) and (B) show concentration-dependent inhibition of TMPRSS2 and plasmin activities by pLF1 but not by LF after 30 min and 4 h. Values of $p < 0.05$, $p < 0.005$, $p < 0.0005$, $p < 0.0001$ (as indicated) were considered to be significant or highly significant, respectively.

terminal peptide pLF1 significantly reduced SARS-CoV-2 infection by $\approx 40\%$ when used at 40 $\mu\text{g/mL}$, while the other two peptides failed to do so, although some non-significant reduction was observed at 40 $\mu\text{g/mL}$ (Figure 3A). pLF1 also showed some inhibitory potential at 20 $\mu\text{g/mL}$ ($\approx 30\%$ inhibition), but the differences were not significant. The control peptide pCTR did not show any inhibitory potential. Of note, the peptides did not show any cytotoxic effects when incubated with Vero cells in the absence of the virus (Supplementary Figure 1).

When we repeated the assay with the human lung cell line Calu-3 that highly expresses TMPRSS2 (6), from the peptides

tested, only pLF1 was able to significantly inhibit SARS-CoV-2 infection by $\approx 45\%$ at both concentrations used (Figure 3B). Interestingly, although full-length LF was not able to block TMPRSS2 activity (Figure 1A), it prevented infection of Vero cells by $\approx 38\%$ when used at 40 $\mu\text{g/mL}$ (Figure 3A), and seemed even more potent in Calu-3 cells, where $\approx 60\text{--}70\%$ inhibition was observed (Figure 3B). This might be likely attributed to LF-mediated blockade of cell-surface HSPGs that aid coronavirus infection (3). Hence, LF seems to obstruct the cell entry of SARS-CoV-2 *via* at least two independent mechanisms.

Biologically active natural peptides, called lactoferricins (LFCs), with antiviral and antibacterial activities are

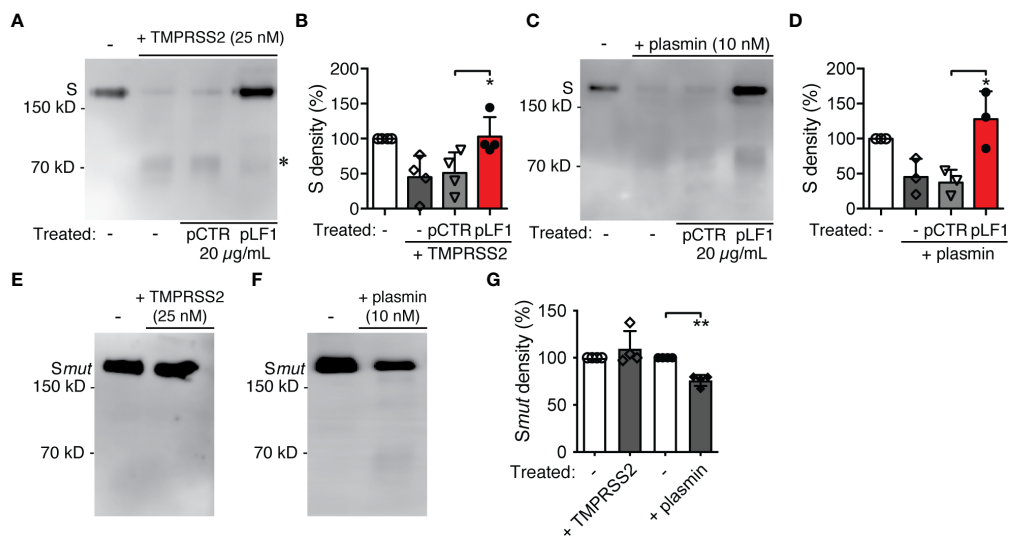


FIGURE 2

Effect of LF and the LF-derived peptides on SARS-CoV-2 S protein proteolytic processing. (A) The purified recombinant 6x-His-tagged S protein was exposed to TMPRSS2 with or without pLF1 or pCTR at 37°C in Tris-HCl buffer for 2 h. The digestion of the S protein was analyzed by immunoblotting of the reaction mixtures followed by an incubation with the specific anti-6x-His mAb. Upon cleavage by TMPRSS2, a digestion product of the S protein of about 75 kD became visible (marked by *). (B) Densitometric quantifications of the proteolytic processing of the S protein by TMPRSS2. Peptide pCTR served as a control. Four independent immunoblotting experiments were evaluated. The bands corresponding to the full-length S protein in the absence of TMPRSS2 were set as a relative maximum of 100%. The immunoblots were quantified by the AzureSpot software. (C) Purified recombinant 6x-His-tagged S protein was exposed to plasmin instead of TMPRSS2 and treated afterwards as in (A). (D) Densitometric quantifications of the proteolytic processing of the S protein by plasmin. Peptide pCTR served as a control. Densitometric evaluation of three independent immunoblotting experiments was performed as in (B). (E-G) The purified recombinant 8x-His-tagged mutated S protein was treated in *in vitro* proteolysis assay with TMPRSS2 (E) and plasmin (F) as in (A, C), and the cleavage (G) was evaluated as in (B, D). Values of $p < 0.05$, $p^{**} < 0.005$ (as indicated) were considered to be significant.

physiologically produced from the N-terminal region of LF upon cleavage by pepsin (12, 13). Therefore, we tested whether LFCs would display a similar inhibitory effect towards TMPRSS2 as the synthetic peptide pLF1. To yield LFC from intact recombinant human LF, we optimized the cleavage conditions (Figure 4A) and chose 60 min incubation in 72 mM HCl and 10% pepsin (per amount of LF) for the subsequent purification. Due to the strong positive charge of LFCs, we used cation exchange chromatography (Figure 4B). The fraction A6, eluted at relatively high conductivity (73–81 mS/cm), was supposed to contain the peptide with the highest isoelectric point. A prominent peptide with an apparent molecular size below 10 kD present in fraction A6 was then analyzed by MALDI-TOF MS. Predominant ions present in spectra corresponded to a peptide with the neutral mass of 5738.1 Da, which was in a good agreement with the published peptide mass of the human LFC spanning 49 amino acids from the N-terminus of mature human LF (21).

An *in vitro* proteolytic activation assay with the fluorogenic substrate Boc-Gln-Ala-Arg-AMC showed that the isolated LFC displayed an inhibitory effect on TMPRSS2 comparable to that of pLF1 (Figure 4C). Accordingly, the isolated LFC reduced the infection rate of replication-competent SARS-CoV-2 in Vero cells (Figure 4D).

Taken together, our data strongly indicate that the N-terminal peptide fragment of LF, LFC, inhibits cell entry of SARS-CoV-2 through blocking TMPRSS2-mediated virus priming.

Discussion

As the global threat of the COVID-19 pandemic persists, it becomes necessary to complement standard treatment protocols and support a vaccine campaign with new causative therapeutics. Virus priming by TMPRSS2 is crucial for the cell entry of SARS-CoV-2, and represents a promising therapeutic target.

Here, we show that the N-terminus of LF contributes to the defense against SARS-CoV-2 infection *via* blockade of TMPRSS2: both the N-terminal synthetic peptide (designed by us and termed pLF1) and the natural N-terminal peptide, produced by controlled pepsin cleavage of LF, inhibit the proteolytic priming of the viral spike protein by TMPRSS2, and subsequently, cell infection by SARS-CoV-2.

We previously found that full-length LF was able to inhibit activation of Plg through hindering the action of urokinase-type

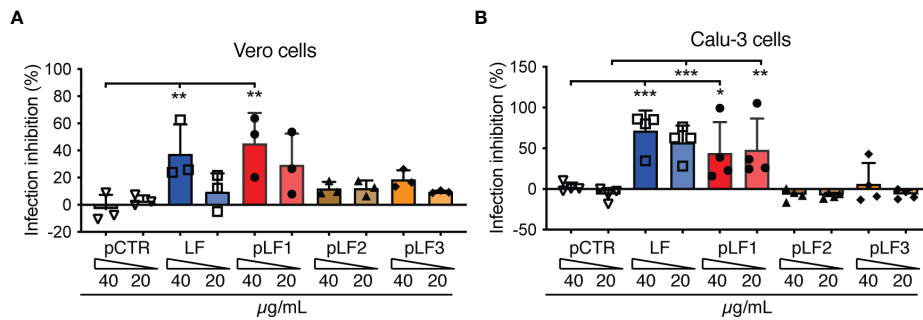


FIGURE 3 Effect of LF and the LF-derived peptides pLF1-pLF3 on the infection capability of SARS-CoV-2. Vero cells (A) or Calu-3 cells (B) grown in 96-well plates were incubated with or without LF, peptides pLF1, pLF2, pLF3 or pCTR for approx. 1 h and then infected with the authentic SARS-CoV-2 (300 TCID50/well). After 48 h, the cells were fixed and the infection rate was assessed by In-Cell ELISA. Values show mean inhibitory capacity of LF and the indicated peptides ± SD from three (A) or four (B) independent experiments. $p < 0.05$, $p^{**} < 0.005$, $p^{***} < 0.0005$. Significance was evaluated by two-way ANOVA with Dunnett’s multiple comparisons post-test.

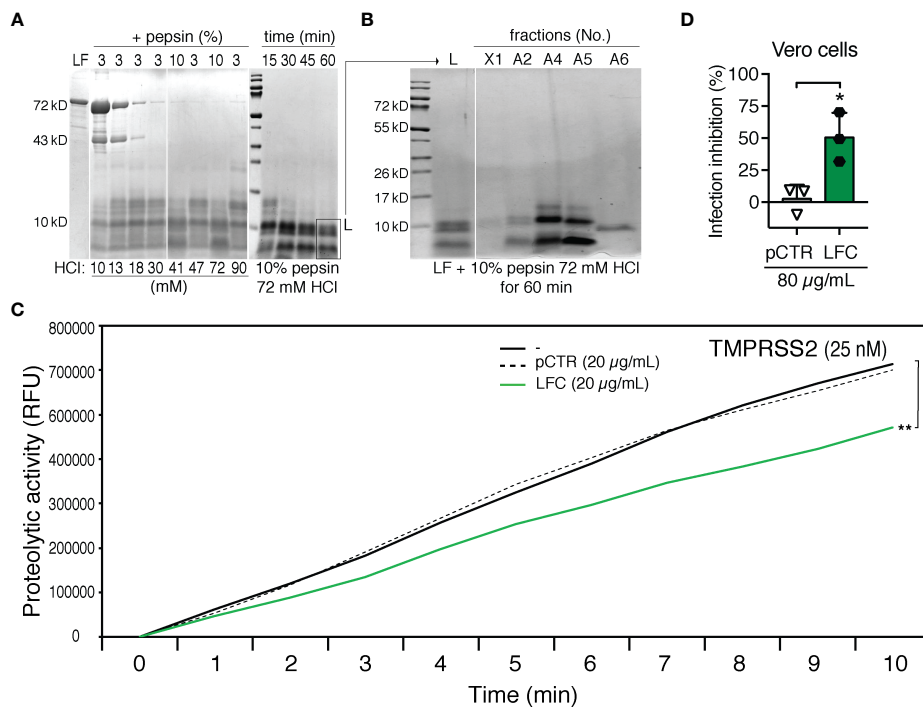


FIGURE 4 Generation and testing of human LFC. (A) Optimizations of HCl and pepsin concentrations (mM and % (w/w), respectively) on LF cleavage. LF (10.5 mg/mL) was exposed to pepsin (3% or 10% per amount of LF) and HCl (10-90 mM, as indicated) for 30 min (left panel) or various time points (15, 30, 45 or 60 min, right panel) at 37°C. Digestion mixtures were analyzed by 10% tricine-SDS-PAGE and subjected to Coomassie blue staining. (B) Separation of LF cleavage products by cation exchange chromatography. Individual fractions were analyzed by 10% tricine-SDS-PAGE and subjected to Coomassie blue staining: L – digestion mixture, X1 - material not captured on the column, A2, A4, A5, A6 - eluted fractions. (C) Effect of LFC (fraction A6) on the activity of TMPRSS2. Proteolytic activity of TMPRSS2 was measured with or without LFC or pCTR at 37°C in Tris-HCl buffer using the fluorogenic substrate Boc-Gln-Ala-Arg-AMC. The reaction was monitored using an ELISA reader for the indicated time intervals. (D) Effect of LFC on the infection capability of SARS-CoV-2. Vero cells were incubated with or without LFC or pCTR (both 80 µg/mL) for approx. 1 h, and then infected with the authentic SARS-CoV-2 (300 TCID50/well; MOI ≈ 0.02). After 48 h, the cells were fixed and the infection rate was assessed by In-Cell ELISA. Values show mean inhibitory capacity of LFC and pCTR ± SD from three independent experiments. $p < 0.05$.

plasminogen activator (uPA), a Plg activator. In contrast, uPA-independent Plg conversion by the bacterial enzyme streptokinase was not affected by LF (11). According to our mapping studies, LF binds to Plg *via* its highly cationic N-terminal region, corresponding to LFC and pLF1 (11). We show that pLF1, but neither full-length LF nor a control peptide (pCTR), was able to inhibit even the intrinsic proteolytic activity of active plasmin. Similarly, only pLF1 but neither full-length LF nor pCTR inhibited the proteolytic activity of closely related TMPRSS2. These findings imply that LF and its N-terminal fragment exploit different inhibitory mechanisms, while LF blocks conversion of inactive Plg to plasmin, the N-terminal peptide pLF1 displays its protease inhibitory effect directly on active plasmin and TMPRSS2. The concentration dependence of inhibition suggests a non-competitive inhibitory mechanism whereby the binding of pLF1 to these active proteases might allosterically decrease the enzyme catalytic rate.

The human glycoprotein LF is synthesized by exocrine glands and is present at high concentrations in secretory body fluids, particularly in milk, but also within inflammatory granules of neutrophils. From the beginning of the pandemic, LF has been recognized as a potential drug candidate (22, 23), and recently, it was found to inhibit SARS-CoV-2 infection *in vitro* (24). Moreover, in a clinical study, supplementary LF treatment significantly reduced COVID-19 symptoms (25). This effect was mainly attributed to its immunomodulatory properties (26).

In our experiments, LF did not block TMPRSS2 activity, yet it prevented SARS-CoV-2 infection. This effect thus might be due to the LF-mediated blockade of HSPGs, since previous research revealed that LF inhibited the SARS-CoV-1 infection through blocking the interaction between the S protein and HSPGs (3). Interestingly, the LF binding to both heparin and HSPGs was observed previously, and it was proposed that the N-terminal region of LF was involved in the binding, thereby inhibiting cell infection by several human coronaviruses, including SARS-CoV-2 (27, 28). Hence, LF and its derived bioactive peptides seem to hinder the cell entry of SARS-CoV-2 through various mechanisms. Additionally, LF appears to inhibit SARS-CoV-2 also at the post-cell entry stage, since it was reported that LF treatment led to e. g. enhancement of interferon responses (24), inhibition of viral replication (29), or maintenance of iron homeostasis (30). Whether the N-terminal region of LF shares some of these antiviral mechanisms with full-length LF, remains to be determined in future studies.

Several biologically active natural peptides derived from the N-terminus of both bovine and human LF by pepsin cleavage, termed lactoferricins (LFCs), were described (13, 21, 31). LFCs possess antibacterial and antiviral activities (32) and their putative activity against SARS-CoV-2 was predicted by simulation (33). Here we report that human LFC as well as the shorter pLF1 peptide from the N-terminal LF region

corresponding to LFC, were able to inhibit SARS-CoV-2 infection in Vero and Calu-3 cells to around 40-50%. It has been reported that SARS-CoV-2 can employ in both cell lines also an endosomal pathway for entry, wherein the SARS-CoV-2 S protein is primed by the cysteine protease cathepsin L (6, 15, 34, 35), which is likely the reason why we have not observed full virus inhibition by the LF-derived N-terminal peptides.

On an equimolar level, the full-length LF may be more potent than peptides. The differences between full-length LF and LF-derived peptides may be attributed to the changes in the peptide secondary structures after their release from the compact LF molecule so that it is not possible for peptides to fold into the original conformation (36). Notably, the intestinal mucosa was shown to contain ACE2 and TMPRSS2 molecules, therefore it is not surprising that SARS-CoV-2 efficiently infects gastrointestinal tissue (37, 38). On this basis, the LFC-mediated inhibition of SARS-CoV-2 infection may be of special relevance under intestinal proteolytic conditions wherein the intact LF is not present.

In addition to TMPRSS2, also other host serine proteases were proposed as therapeutic targets to block SARS-CoV-2 cell entry (4, 5, 8, 9, 39, 40). Here, we show that peptide pLF1 derived from the N-terminus of LF inhibits processing of the S protein not only by TMPRSS2 but also by plasmin. Notably, a high plasmin level is considered as risk factor for development of COVID-19 after SARS-CoV-2 infection (41). Interestingly, the influenza virus hemagglutinin variant with a Ser-Tyr substitution in the cleavage site was shown to be preferentially cleaved by plasmin (42). Thus, host serine protease redundancy to exert SARS-CoV-2 priming might also contribute to enhanced fitness of emerging variants.

Representative data on LFC levels in human sera are not available. However, since LFCs are digestion products derived from LF, data on serum LF levels might be correlative. According to our unpublished measurements and also published studies of others, LF levels in blood sera of healthy donors may vary within a dynamic range up to $\mu\text{g/mL}$ values (43), which makes the effective concentrations around IC₅₀ achievable.

LF and its bioactive peptides offer health benefits also beyond newborns. Cow-, goat- or sheep milk and cheese are common components of diet for adults. However, LF derived from various mammalian species may show different anti-SARS-CoV-2 abilities (29). Depiction of their inhibitory capacities against TMPRSS2 remains for future studies.

Collectively, our results reveal that not only full-length human LF but also its bioactive digestion products may be protective against COVID-19, however, *via* different mechanisms, which can produce synergic therapeutic or prophylactic effects. LF is present at high concentrations in milk and other dairy products, as well as in food supplements. Orally administered LF endows a major clinical benefit in human, particularly neonatal medicine (44), and it is considered safe and without adverse effects (45). This makes

LF a cheap and widely available candidate for supplementary therapy in management of COVID-19.

Materials and methods

Peptides

The peptides derived from human LF were synthesized by Peptide 2.0 (Chantilly, VA). The sequences of the 19-residue synthetic peptides were as follows: GRRRSVQWCAVSQEATKC (N-terminal pLF1, residues 1-19), EDAIWNLLRQAQEKFGKDK (middle pLF2, residues 264-282), NLKKCSTSPLEACEFLRK (C-terminal pLF3, residues 673-691), and NFRTKSCPLELAKELKLS (pCTR, a scrambled variant of pLF3) (11). Numbering of the LF peptides refers to a mature secreted form of the representative LF isoform P02788-1 (www.uniprot.org).

In vitro proteolysis assay

The proteolytic activities of plasmin (10 nM; from human plasma; #10602361001, Roche Diagnostics GmbH, Mannheim, Germany), trypsin (10 nM; from bovine pancreas; #T1005, Sigma-Aldrich, St. Louis, MO), elastase (20 nM; from porcine pancreas; #E1250, Sigma-Aldrich) and TMPRSS2 (25 nM; recombinant protein produced in mammalian cells; #MBS1193731, MyBioSource, San Diego, CA) were measured in a Nunc black fluorescence-based cell assay plate (Sigma-Aldrich) in Tris-HCl buffer (20 mM, pH 8.0, 150 mM NaCl). The proteases were incubated with or without inhibitory and control compounds at 37°C for 30 min, and then the fluorogenic substrate (Boc-Gln-Ala-Arg-AMC; 25 μM; #BML-P237, ENZO Life Sciences, Lörrach, Germany) was added. The reaction was measured using an ELISA plate reader (Synergy H1 BioTek microplate reader, Winooski, Vermont, U.S., or TECAN GENios, GMI, USA) under the excitation wavelength of 380 nm and the emission wavelength of 460 nm at the indicated time points.

Optionally (Figure 1B, inset), purified active plasmin (10 mU/mL) was coated in PBS directly on a 96-well Falcon transparent plate for 2 h at 37°C. The wells were then blocked with 1% BSA, washed, and then incubated in PBS at 37°C with the chromogenic plasmin substrate S-2251 (0.8 mM, D-Val-Leu-Lys-pNA, CoaChrom Diagnostica). In this case, the absorbance change at 405 nm was monitored at different time points by using an ELISA plate reader (SpectraMax M5, Molecular Devices).

In the SARS-CoV-2 S protein digestion assay, purified recombinant 6x-His-tagged S protein (1 μg; #REC31868, NativeAntigen, Kidlington, UK) was exposed to TMPRSS2 (25 nM) or plasmin (10 nM) with or without inhibitory and control compounds for 120 min at 37°C in Tris-HCl buffer (20 mM, pH 7.5, 150 mM NaCl). The reaction was stopped by adding SDS-

PAGE sample buffer, the reaction mixtures were then boiled and analyzed by immunoblotting with a specific anti-6x-His tag monoclonal antibody (mAb) (#631212, Clontech, Heidelberg, Germany).

Preparation of the mutated S protein

Prefusion-stabilized SARS-CoV-2 S protein ectodomain (46) (residues 1–1208 from GenBank: MN908947), with proline substitutions at residues 986 and 987, a “GSAS” substitution at the furin cleavage site residues 682–685, a C-terminal T4 fibrin trimerization motif, an HRV3C protease cleavage site, a Twin-Strep-tag and an 8x-His tag, was expressed in CHO cells and purified as described previously (47). Briefly, the S protein secreted to cell media was captured on a 5 ml His-Trap affinity column (Cytiva, Marlborough, MA, USA), eluted with 0.5 M imidazole in 20 mM sodium phosphate buffer, pH 7.4 and further purified on the Strep-Tactin[®] media (IBA Lifesciences GmbH, Göttingen, Germany) as described by the manufacturer, using 10 mM desthiobiotin (IBA Lifesciences) as an elution reagent. The purified S protein was concentrated by ultrafiltration and buffer-exchanged into PBS on a 5 ml HiTrap Desalting column (Cytiva). The concentration was determined by UV absorbance at 280 nm. Finally, the S protein was sterile-filtered and stored at -20°C.

Generation of LFC and MALDI-TOF MS

Recombinant human LF (L1294, Sigma-Aldrich) was digested by pepsin (from porcine stomach mucosa; #P6887, Sigma-Aldrich). To a LF solution (10.5 mg/mL) in 150 mM NaCl, pepsin (3% or 10% per amount of LF) and HCl (10, 13, 18, 30, 41, 47, 72 or 90 mM) were added for various times (15, 30, 45 or 60 min). Upon the optimal cleavage condition (72 mM HCl and 10% pepsin for 60 min at 37°C), LF was completely cleaved into short peptides. The resulting digestion mixture was purified by cation exchange chromatography using a 1 mL Mono S column (GE Healthcare). Gradient of ammonium carbonate (20 to 1500 mM) was used for elution. Samples were analyzed by 10% tricine-SDS-PAGE and subjected to Coomassie blue staining. A fraction eluted at 73-81 mS/cm conductivity was dried and incubated at 60°C overnight to remove the ammonium carbonate. The sample was dissolved in PBS and the concentration was determined from the absorbance at 280 nm using an extinction coefficient of 11250 M⁻¹cm⁻¹. 40% ACN/0.1% TFA was used for dissolving the sample before MALDI analysis. Equal volume of sample and alpha-cyano-4-hydroxycinnamic acid (HCCA) matrix solution (10 mg/mL in 70% ACN/0.1% TFA) was mixed on MALDI target plate. MALDI analysis was performed in positive mode. Single and double charged ions present in spectra corresponded to a peptide

with the neutral mass of 5738.1 Da, which was in good agreement with the published human LFC peptide mass (sequence GRRRRSVQWCAVSQPEATKCFQWQRNMRKV RGPPVSCIKRDSPIQCIQA) (21).

Immunoblotting

Immunoblotting was performed as described previously (48). Briefly, samples obtained from *in vitro* proteolysis or binding assays were analyzed by electrophoresis on an 8% SDS-polyacrylamide gel (SDS-PAGE) followed by a transfer at constant voltage (15 V) to an Immobilon polyvinylidene difluoride membrane (Millipore Co., Bedford, MA). The membranes were blocked using 4% nonfat milk and immunostained with an appropriate mAb followed by a corresponding secondary HRP-conjugate. For visualization of proteins, the chemiluminescence image analyzer Azure 280 (AzureBiosystems, Dublin, CA) was used. Densitometric quantifications of corresponding bands were done by means of AzureSpot software.

SARS-CoV-2 infection and In-Cell ELISA

The African green monkey kidney-derived Vero cells (ATCC CCL-81, provided by Prof. Sylvia Knapp, Medical University of Vienna) or human lung adenocarcinoma Calu-3 cells (ATCC HTB-55, provided by Prof. Walter Berger, Medical University of Vienna) were seeded into 96-well flat-bottom plates (1×10^4 cells for Vero or 2×10^4 cells for Calu-3, 80 μ l/well) in Dulbecco's Modified Eagle's medium (DMEM), high glucose, with GlutaMAX and sodium pyruvate (Gibco/Thermo Fisher Scientific, Waltham, MA USA) supplemented with 10% fetal calf serum (FCS, Biowest, Nuaille, France), 1% MEM non-essential amino acids solution, 100 U/mL penicillin and 100 μ g/mL streptomycin (all latter from Gibco/Thermo Fisher Scientific). On the next day, tested peptides, LF and controls were diluted in DMEM medium with reduced serum (2% FCS) in a separate plate so that the concentration was 1.33-fold higher than final. Ninety μ l of the solution was used to pretreat seeded cells (old medium was discarded) for approx. 40-60 min. During the incubation time, cells were transferred to the BSL3 facility of the Medical University of Vienna and then infected with 30 μ l (300 TCID₅₀/well; multiplicity of infection (MOI) \approx 0.02) of the authentic SARS-CoV-2 isolate BetaCoV/Munich/BavPat1/2020 [kindly provided by Christian Drosten, Charité, Berlin (49), and distributed by the European Virology Archive (Ref-SKU: 026V-03883)] that was diluted to 1×10^4 TCID₅₀/mL in DMEM/2% FCS. Cells were then incubated at 37°C. After 48 h, cells were fixed by adding 45 μ l/well 37% formaldehyde for 20 min.

Supernatants were then aspirated and the entire plate was fixed in fresh 5% formaldehyde in PBS for 30 min. Next, the formaldehyde was removed, the cells were washed with PBS, permeabilized using 0.1% Triton X-100 in PBS and blocked with blocking buffer (10% FCS in PBS+0.05% Tween-20). Subsequently, the cells were stained by indirect immunofluorescence using a rabbit anti-SARS-CoV-2 nucleocapsid mAb (40143-R019, SinoBiological, Beijing, China, diluted 1:15000 in blocking buffer) followed by a goat anti-rabbit-HRP conjugate (170-6515, Bio-Rad, Hercules, CA USA, diluted 1:10000 in blocking buffer). In-Cell ELISA was then developed using DY999 substrate solution according to the manufacturer's recommendations (R&D Systems, Minneapolis, MN USA) and measured at 450 nm (and at 630 nm to assess the background) using a Mithras multimode plate reader (Berthold Technologies, Bad Wildbad, Germany). To calculate percent inhibition of infection in each well, the following formula was used: $100 - [(X - \text{average of 'no virus' wells}) / (\text{average of 'virus only' wells} - \text{average of 'no virus' wells}) * 100]$, where X is the background-subtracted read for each well, as we did previously (50, 51).

Cytotoxicity assay

Vero cells were seeded into 96-well flat-bottom plates (1×10^4 cells, 80 μ l/well) in DMEM medium supplemented with 10% FCS, antibiotics, and non-essential amino acids. On the day of the assay, the medium was exchanged for the reduced serum supplemented DMEM (DMEM/2% FCS) with the peptides or a vehicle only at the designated concentration (100 μ l/well). As a positive control, 30% DMSO in DMEM/2% FCS was used. Negative control cells were incubated in DMEM/2% FCS only. Two days (48 h) later, cell viability was assessed as we did previously (52) using the EZ4U cell proliferation and cytotoxicity assay substrate (Biomedica Immunoassays, Vienna, Austria).

Statistical analysis

All experiments were performed at least three times in at least duplicates. The data were expressed as mean values with standard deviations (SD). Graphing and statistical significance evaluation (using a Student's t-test or one-way ANOVA with Dunnett's multiple comparisons post-test, unless stated otherwise) was done in Prism 9 for MacOS. Values of $p < 0.05$, $p^{**} < 0.005$, $p^{***} < 0.0005$, $p^{****} < 0.0001$ (as indicated) were considered to be significant or highly significant, respectively. Relative IC₅₀ values were determined also in Prism by a 4PL nonlinear regression curve fit.

Data availability statement

The original contributions presented in the study are included in the article/**Supplementary Material**. Further inquiries can be directed to the corresponding authors.

Author contributions

VL, AO-R and RS conceived and designed the experiments. VL, GO and RP made biochemical analyses, AO-R, LG, and GT, made cell infection assays, RS, NJ, PH made chromatography purification, PB performed mass spectrometry, HS contributed with ideas, comments and materials. VL wrote the paper. All authors read and corrected the manuscript. All authors contributed to the article and approved the submitted version.

Funding

This work was supported by grants of the Science and Technology Assistance Agency of the Slovak Republic (APVV-16-0452, APVV-20-0513), of the Slovak Grant Agency VEGA (2/0020/17, 2/0152/21) and of the Austrian Science Fund (FWF; P 34253-B).

Acknowledgments

The authors thank Prof. Sylvia Knapp, Dr. Riem Gawish and the other Knapp lab members (Medical University of Vienna,

Department of Medicine I, Research Laboratory of Infection Biology, Vienna, Austria) for the support and constructive discussions. The authors also thank Prof. Walter Berger, Medical University of Vienna, Center for Cancer Research, Vienna, Austria) for providing Calu-3 cells.

Conflict of interest

The authors declare that the research was conducted in the absence of any commercial or financial relationships that could be construed as a potential conflict of interest.

Publisher's note

All claims expressed in this article are solely those of the authors and do not necessarily represent those of their affiliated organizations, or those of the publisher, the editors and the reviewers. Any product that may be evaluated in this article, or claim that may be made by its manufacturer, is not guaranteed or endorsed by the publisher.

Supplementary material

The Supplementary Material for this article can be found online at: <https://www.frontiersin.org/articles/10.3389/fimmu.2022.958581/full#supplementary-material>

References

- Li W, Moore MJ, Vasilieva N, Sui J, Wong SK, Berne MA, et al. Angiotensin-converting enzyme 2 is a functional receptor for the sars coronavirus. *Nature* (2003) 426(6965):450–4. doi: 10.1038/nature02145
- Zhou P, Yang XL, Wang XG, Hu B, Zhang L, Zhang W, et al. A pneumonia outbreak associated with a new coronavirus of probable bat origin. *Nature* (2020) 579(7798):270–3. doi: 10.1038/s41586-020-2012-7
- Lang J, Yang N, Deng J, Liu K, Yang P, Zhang G, et al. Inhibition of SARS pseudovirus cell entry by lactoferrin binding to heparan sulfate proteoglycans. *PLoS One* (2011) 6(8):e23710. doi: 10.1371/journal.pone.0023710
- Fuentes-Prior P. Priming of SARS-CoV-2 S protein by several membrane-bound serine proteinases could explain enhanced viral infectivity and systemic covid-19 infection. *J Biol Chem* (2021) 296:100135. doi: 10.1074/jbc.REV120.015980
- Dessie G, Malik T. Role of serine proteases and host cell receptors involved in proteolytic activation, entry of SARS-CoV-2 and its current therapeutic options. *Infect Drug Resist* (2021) 14:1883–92. doi: 10.2147/IDR.S308176
- Koch J, Uckelej ZM, Doldan P, Stanifer M, Boulant S, Lozach PY. TMPRSS2 expression dictates the entry route used by SARS-CoV-2 to infect host cells. *EMBO J* (2021) 40(16):e107821. doi: 10.15252/embj.2021107821
- Gioia M, Ciaccio C, Calligari P, De Simone G, Sbardella D, Tundo G, et al. Role of proteolytic enzymes in the COVID-19 infection and promising therapeutic approaches. *Biochem Pharmacol* (2020) 182:114225. doi: 10.1016/j.bcp.2020.114225
- Kaur U, Chakrabarti SS, Ojha B, Pathak BK, Singh A, Saso L, et al. Targeting host cell proteases to prevent SARS-CoV-2 invasion. *Curr Drug Targets* (2021) 22(2):192–201. doi: 10.2174/1389450121666200924113243
- Muller P, Maus H, Hammerschmidt SJ, Knaff P, Mailander V, Schirmeister T, et al. Interfering with host proteases in SARS-CoV-2 entry as a promising therapeutic strategy. *Curr Med Chem* (2022) 29(4):635–65. doi: 10.2174/0929867328666210526111318
- Huggins DJ. Structural analysis of experimental drugs binding to the SARS-CoV-2 target TMPRSS2. *J Mol Graph Model* (2020) 100:107710. doi: 10.1016/j.jmgm.2020.107710
- Zwirzitz A, Reiter M, Skrabana R, Ohradanova-Repic A, Majdic O, Gutekova M, et al. Lactoferrin is a natural inhibitor of plasminogen activation. *J Biol Chem* (2018) 293(22):8600–13. doi: 10.1074/jbc.RA118.003145
- Wakabayashi H, Takase M, Tomita M. Lactoferricin derived from milk protein lactoferrin. *Curr Pharm design* (2003) 9(16):1277–87. doi: 10.2174/1381612033454829
- Zarzosa-Moreno D, Avalos-Gomez C, Ramirez-Textcalco LS, Torres-Lopez E, Ramirez-Mondragon R, Hernandez-Ramirez JO, et al. Lactoferrin and its derived peptides: An alternative for combating virulence mechanisms developed by pathogens. *Molecules* (2020) 25(24):5763. doi: 10.3390/molecules25245763
- Kawase M, Shirato K, van der Hoek L, Taguchi F, Matsuyama S. Simultaneous treatment of human bronchial epithelial cells with serine and cysteine protease inhibitors prevents severe acute respiratory syndrome coronavirus entry. *J Virol* (2012) 86(12):6537–45. doi: 10.1128/JVI.00094-12

15. Hoffmann M, Kleine-Weber H, Schroeder S, Kruger N, Herrler T, Erichsen S, et al. SARS-CoV-2 cell entry depends on ACE2 and TMPRSS2 and is blocked by a clinically proven protease inhibitor. *Cell* (2020) 181(2):271–80.e8. doi: 10.1016/j.cell.2020.02.052
16. Glowacka I, Bertram S, Muller MA, Allen P, Soilleux E, Pfefferle S, et al. Evidence that TMPRSS2 activates the severe acute respiratory syndrome coronavirus spike protein for membrane fusion and reduces viral control by the humoral immune response. *J Virol* (2011) 85(9):4122–34. doi: 10.1128/JVI.02232-10
17. Jackson CB, Farzan M, Chen B, Choe H. Mechanisms of SARS-CoV-2 entry into cells. *Nat Rev Mol Cell Biol* (2022) 23(1):3–20. doi: 10.1038/s41580-021-00418-x
18. Essalmani R, Jain J, Susan-Resiga D, Andreo U, Evagelidis A, Derbali RM, et al. Distinctive roles of furin and TMPRSS2 in SARS-CoV-2 infectivity. *J Virol* (2022) 96(8):e0012822. doi: 10.1128/jvi.00128-22
19. Tang T, Jaimes JA, Bidon MK, Straus MR, Daniel S, Whittaker GR. Proteolytic activation of SARS-CoV-2 Spike at the S1/S2 boundary: Potential role of proteases beyond furin. *ACS Infect Dis* (2021) 7(2):264–72. doi: 10.1021/acscinfdis.0c00701
20. Matsuyama S, Nao N, Shirato K, Kawase M, Saito S, Takayama I, et al. Enhanced isolation of SARS-CoV-2 by TMPRSS2-expressing cells. *Proc Natl Acad Sci U.S.A.* (2020) 117(13):7001–3. doi: 10.1073/pnas.2002589117
21. Hunter HN, Demcoe AR, Jenssen H, Gutteberg TJ, Vogel HJ. Human lactoferrin is partially folded in aqueous solution and is better stabilized in a membrane mimetic solvent. *Antimicrob Agents Chemother* (2005) 49(8):3387–95. doi: 10.1128/AAC.49.8.3387-3395.2005
22. Naidu SAG, Clemens RA, Pressman P, Zaigham M, Davies KJA, Naidu AS. COVID-19 during pregnancy and postpartum: Antiviral spectrum of maternal lactoferrin in fetal and neonatal defense. *J Diet Suppl* (2022) 19(1):78–114. doi: 10.1080/19390211.2020.1834047
23. Campione E, Cosio T, Rosa L, Lanna C, Di Girolamo S, Gaziano R, et al. Lactoferrin as protective natural barrier of respiratory and intestinal mucosa against coronavirus infection and inflammation. *Int J Mol Sci* (2020) 21(14):4903. doi: 10.3390/ijms21144903
24. Mirabelli C, Wotrting JW, Zhang CJ, McCarty SM, Fursmid R, Pretto CD, et al. Morphological cell profiling of SARS-CoV-2 infection identifies drug repurposing candidates for COVID-19. *Proc Natl Acad Sci U.S.A.* (2021) 118(36):e2105815118. doi: 10.1073/pnas.2105815118
25. Rosa L, Tripepi G, Naldi E, Aimati M, Santangeli S, Venditto F, et al. Ambulatory COVID-19 patients treated with lactoferrin as a supplementary antiviral agent: A preliminary study. *J Clin Med* (2021) 10(18):4276. doi: 10.3390/jcm10184276
26. Legrand D, Ellass E, Carpentier M, Mazurier J. Interactions of lactoferrin with cells involved in immune function. *Biochem Cell Biol* (2006) 84(3):282–90. doi: 10.1139/o06-045
27. Hu Y, Meng X, Zhang F, Xiang Y, Wang J. The in vitro antiviral activity of lactoferrin against common human coronaviruses and SARS-CoV-2 is mediated by targeting the heparan sulfate co-receptor. *Emerg Microbes Infect* (2021) 10(1):317–30. doi: 10.1080/22221751.2021.1888660
28. Shimazaki K, Tazume T, Uji K, Tanaka M, Kumura H, Mikawa K, et al. Properties of a heparin-binding peptide derived from bovine lactoferrin. *J Dairy Sci* (1998) 81(11):2841–9. doi: 10.3168/jds.S0022-0302(98)75843-6
29. Lai X, Yu Y, Xian W, Ye F, Ju X, Luo Y, et al. Identified human breast milk compositions effectively inhibit SARS-CoV-2 and variants infection and replication. *iScience* (2022) 25(4):104136. doi: 10.1016/j.isci.2022.104136
30. Naidu SAG, Clemens RA, Naidu AS. SARS-CoV-2 infection dysregulates host iron (Fe)-redox homeostasis (Fe-R-H): Role of Fe-redox regulators, ferroptosis inhibitors, anticoagulants, and iron-chelators in COVID-19 control. *J Diet Suppl* (2022), 1–60. doi: 10.1080/19390211.2022.2075072
31. Bellamy W, Takase M, Wakabayashi H, Kawase K, Tomita M. Antibacterial spectrum of lactoferrin B, a potent bactericidal peptide derived from the N-terminal region of bovine lactoferrin. *J Appl bacteriology* (1992) 73(6):472–9. doi: 10.1111/j.1365-2672.1992.tb05007.x
32. Gifford JL, Hunter HN, Vogel HJ. Lactoferrin: A lactoferrin-derived peptide with antimicrobial, antiviral, antitumor and immunological properties. *Cell Mol Life Sci* (2005) 62(22):2588–98. doi: 10.1007/s00018-005-5373-z
33. Zhao W, Li X, Yu Z, Wu S, Ding L, Liu J. Identification of lactoferrin-derived peptides as potential inhibitors against the main protease of SARS-CoV-2. *Lebensm Wiss Technol* (2022) 154:112684. doi: 10.1016/j.lwt.2021.112684
34. Zhao MM, Yang WL, Yang FY, Zhang L, Huang WJ, Hou W, et al. Cathepsin L plays a key role in SARS-CoV-2 infection in humans and humanized mice and is a promising target for new drug development. *Signal Transduct Target Ther* (2021) 6(1):134. doi: 10.1038/s41392-021-00558-8
35. Mellott DM, Tseng CT, Drelich A, Fajtova P, Chenna BC, Kostomiris DH, et al. A clinical-stage cysteine protease inhibitor blocks SARS-CoV-2 infection of human and monkey cells. *ACS Chem Biol* (2021) 16(4):642–50. doi: 10.1021/acscchembio.0c00875
36. Peterson NA, Anderson BF, Jameson GB, Tweedie JW, Baker EN. Crystal structure and iron-binding properties of the R210K mutant of the N-lobe of human lactoferrin: Implications for iron release from transferrins. *Biochemistry* (2000) 39(22):6625–33. doi: 10.1021/bi0001224
37. Zang R, Gomez Castro MF, McCune BT, Zeng Q, Rothlauf PW, Sonnek NM, et al. TMPRSS2 and TMPRSS4 promote SARS-CoV-2 infection of human small intestinal enterocytes. *Sci Immunol* (2020) 5(47):eabc3582. doi: 10.1126/sciimmunol.abc3582
38. Xiao F, Tang M, Zheng X, Liu Y, Li X, Shan H. Evidence for gastrointestinal infection of SARS-CoV-2. *Gastroenterology* (2020) 158(6):1831–3.e3. doi: 10.1053/j.gastro.2020.02.055
39. Bojkova D, Bechtel M, McLaughlin KM, McGreig JE, Klann K, Bellinghausen C, et al. Aprotinin inhibits SARS-CoV-2 replication. *Cells* (2020) 9(11):2377. doi: 10.3390/cells9112377
40. Bestle D, Heindl MR, Limburg H, Van Lam van T, Pilgram O, Moulton H, et al. TMPRSS2 and furin are both essential for proteolytic activation of SARS-CoV-2 in human airway cells. *Life Sci Alliance* (2020) 3(9):e202000786. doi: 10.26508/lsa.202000786
41. Ji HL, Zhao R, Matalon S, Matthay MA. Elevated plasmin(ogen) as a common risk factor for COVID-19 susceptibility. *Physiol Rev* (2020) 100(3):1065–75. doi: 10.1152/physrev.00013.2020
42. Tse LV, Marcano VC, Huang W, Pocwierz MS, Whittaker GR. Plasmin-mediated activation of pandemic H1N1 influenza virus hemagglutinin is independent of the viral neuraminidase. *J Virol* (2013) 87(9):5161–9. doi: 10.1128/JVI.00210-13
43. Dikovskaya MA, Trunov AN, Chernykh VV, Korolenko TA. Cystatin C and lactoferrin concentrations in biological fluids as possible prognostic factors in eye tumor development. *Int J Circumpolar Health* (2013) 72. doi: 10.3402/ijch.v72i0.21087
44. Kaur G, Gathwala G. Efficacy of bovine lactoferrin supplementation in preventing late-onset sepsis in low birth weight neonates: A randomized placebo-controlled clinical trial. *J Trop Pediatr* (2015) 61(5):370–6. doi: 10.1093/tropej/fmv044
45. Manzoni P. Clinical benefits of lactoferrin for infants and children. *J Pediatr* (2016) 173 Suppl:S43–52. doi: 10.1016/j.jpeds.2016.02.075
46. Wrapp D, Wang N, Corbett KS, Goldsmith JA, Hsieh CL, Abiona O, et al. Cryo-EM structure of the 2019-nCoV spike in the prefusion conformation. *Science* (2020) 367(6483):1260–3. doi: 10.1126/science.abb2507
47. Kovacech B, Fialova L, Filipcik P, Skrabana R, Zilkova M, Paulenka-Ivanovova N, et al. Monoclonal antibodies targeting two immunodominant epitopes on the Spike protein neutralize emerging SARS-CoV-2 variants of concern. *EBioMedicine* (2022) 76:103818. doi: 10.1016/j.ebiom.2022.103818
48. Ohradanova-Repic A, Machacek C, Donner C, Muhlgraber V, Petrovcikova E, Zahradnikova AJr., et al. The mannose 6-phosphate/insulin-like growth factor 2 receptor mediates plasminogen-induced efferocytosis. *J Leukoc Biol* (2019) 105(3):519–30. doi: 10.1002/JLB.1AB0417-160RR
49. Rothe C, Schunk M, Sothmann P, Bretzel G, Froeschl G, Wallrauch C, et al. Transmission of 2019-nCoV infection from an asymptomatic contact in Germany. *N Engl J Med* (2020) 382(10):970–1. doi: 10.1056/NEJMc2001468
50. Gattinger P, Kratzer B, Tulaeva I, Niespodziana K, Ohradanova-Repic A, Gebetsberger L, et al. Vaccine based on folded receptor binding domain-PreS fusion protein with potential to induce sterilizing immunity to SARS-CoV-2 variants. *Allergy* (2022) 77(8):2431–45. doi: 10.1111/all.15305
51. Wagner A, Garner-Spitzer E, Schotta AM, Orola M, Wessely A, Zwazl I, et al. SARS-CoV-2-mRNA booster vaccination reverses non-responsiveness and early antibody waning in immunocompromised patients - a phase four study comparing immune responses in patients with solid cancers, multiple myeloma and inflammatory bowel disease. *Front Immunol* (2022) 13:889138. doi: 10.3389/fimmu.2022.889138
52. Ohradanova-Repic A, Nogueira E, Hartl I, Gomes AC, Preto A, Steinhuber E, et al. Fab antibody fragment-functionalized liposomes for specific targeting of antigen-positive cells. *Nanomedicine* (2018) 14(1):123–30. doi: 10.1016/j.nano.2017.09.003